Proceedings of the 11th World Congress on Mechanical, Chemical, and Material Engineering (MCM'25)

Paris, France - August, 2025 Paper No. HTFF 118 DOI: 10.11159/htff25.118

# **Evaporative Cooling With Hierarchically Graded Porous Network**

## Xuewei Zhang, Sylvie Lorente,

Mechanical Engineering Department, Villanova University 800 Lancaster Avenue, Villanova, PA, USA Xzhang5@villanova.edu; sylvie.lorente@villanova.edu

**Abstract** - In this work, we show the impact on the heat transfer coefficient of the design of porous network for evaporative cooling. The heat transfer fluid is pumped through the porous network by capillary suction and evaporates at the top surface of the porous system impacted by a high heat flux. If the liquid recesses within the porous system, there is a significant loss of thermal performance. Through a fundamental approach, the study bridges the fluid mechanics aspects of the design of the pore network and the heat transfer that governs the exchanges at the fluid meniscus interface with the ambient.

**Keywords:** Electronics cooling, Evaporative cooling, Two-phase flow, Capillary porous network.

#### 1. Introduction

Miniaturization in electronics comes with higher power densities and subsequently higher needs in temperature control to maintain the reliability and safety of electronic components. In this context, a lot of efforts are placed into two-phase cooling and the promise of superior cooling densities. Capillary pumping is a class of solution by itself because such a solution does not need any mechanical device to drive the heat transfer fluid to the heat source where it can evaporate. This can be obtained with porous materials in which the pore size is small enough to generated suction, pulling the liquid up to the top surface of the material where it can evaporate. Because latent heat is way higher than sensible heat, the heat transfer coefficient obtained with evaporative cooling allows to balance high heat fluxes. The field is vibrant with advances brought on type of heat transfer fluid [1], evaporator [2, 3], and capillary structures [4-6]. One of the biggest challenges in such configuration is the risk of liquid recess within the porous material, in which case the thermal advantage of the solution is lost. This article reviews the methodology developed by our group [7] to design a pore network for evaporation cooling. The objective of the study is to show how a pore network with a graded porosity, i.e. a controlled change in pore channels length and diameter with the height of the porous material, is able to drive the heat transfer liquid (water in the case of this work) all the way to the top surface of the porous material with minimum friction losses. An additional objective is to allow evaporation of the liquid at the very top of the pore network where a heat flux is applied.

#### 2. Model

Assume a sample of porous material in contact with a liquid reservoir at its bottom surface. The liquid can fill the cylindrical pore space thanks to capillary suction. The top surface of the material is hit by a constant heat flux. It is expected that evaporation at the surface of the material will balance the received heat thanks to the liquid latent heat. Figure 1 shows the geometry of the porous system in an example where two pore inlets join in a dendritic fashion and connect to one pore outlet, together with a zoom on the problem description at the top of the material with the interface between liquid (water) and air.

We developed an algorithm on Matlab solving simultaneously the set of equations presented below and searching for the best pore network configuration for a given material porosity. The input data are the porosity, radius of the outlet pore and heat flux reaching the top surface of the porous material. The energy balance writes

$$\dot{m}_{pore}h_{fg} = q_{input}^{"}A_{input} \tag{1}$$

where  $\dot{m}_{pore}$  is the evaporative mass flow rate,  $h_{fg}$  is the latent heat of the fluid,  $q_{input}^{"}$  is the heat flux, and  $A_{input}$  is the elemental area receiving the heat flux. In steady state, the momentum equation (Eq. 2) gives the balances between capillary force, gravity and friction losses, allowing to design the entire pore network when accounting for a relationship between parent channels and children channels (Eq. 3). Additionally, the capillary forces must be able to sustain the flow rate that passes through all channels. This is accounted for by defining a Capillary Strength condition, CS, calculated with Eq. (4).

$$\frac{2\sigma\cos\theta}{r_{outlet}} = \frac{8\mu}{\pi\rho_l} \sum_{\substack{l,\dot{m}_i\\l'_i}} \frac{l_i\dot{m}_i}{r_i^4} + g\rho_l H \tag{2}$$

$$r_3^{\gamma} = r_1^{\gamma} + r_2^{\gamma} \tag{3}$$

$$CS_{1} = \frac{2\sigma\cos\theta}{r_{1}} - \frac{8\mu l_{1}\dot{m}_{1}}{\pi\rho_{1}} - g\rho_{1}v_{D} \ge 0$$
(4)

The set of equations is completed with an evaporation model giving the balance between the local heat flux through the liquid at the meniscus (Eq. 5), and the evaporative heat flux at the interface obtained from the Schrage's equation (Eq. 6).

$$q_I^{"} = k_I \frac{T_W - T_{\delta}(\eta)}{\delta(\eta)} \tag{5}$$

$$q_{e}^{"} = \frac{2\bar{\sigma}}{2 - \bar{\sigma}\sqrt{2\pi R_{g}}} \sqrt{\frac{P_{\delta}(\eta)}{T_{\delta}(\eta)}} - \frac{P_{s}(T_{v})}{\sqrt{T_{v}}}$$

$$(6)$$

where  $k_I$  is the thermal conductivity of the liquid,  $T_{\delta}(\eta)$  is the interface temperature, and  $\delta(\eta)$  is the normal distance from the interface to the wall,  $\bar{\sigma}$  is the accommodation coefficient,  $R_g$  is the gas constant,  $h_{fg}$  is the latent heat of liquid,  $P_s(T_v)$  is the saturation pressure of the vapor at temperature  $T_v$ . The interface pressure  $P_{\delta}(\eta)$  is obtained from the extended Kelvin equation [26].

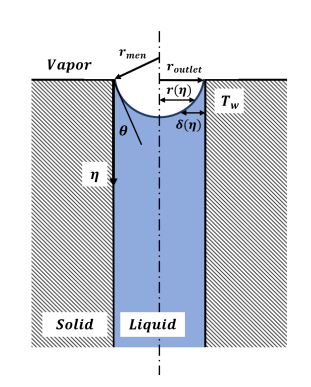
$$P_{\delta}(\eta) = P_{s}(T_{\delta}) exp \left[ \frac{P_{\delta}(\eta) - P_{s}(T_{\delta}) + P_{d} - P_{c}}{\rho_{l} R_{g} T_{\delta}(\eta)} \right]$$
(7)

where  $P_s(T_\delta)$  is the saturation pressure at the temperature  $T_\delta$ ,  $\rho_I$  is the liquid density,  $P_d$  is the disjoining pressure. The capillary pressure  $P_c$  is given by

$$P_c = \frac{2\sigma}{r_{men}} \tag{8}$$

where  $\sigma$  is surface tension.





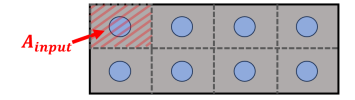


Fig.1: Porous material and its elemental structures (left), and geometry at the water/air interface at the top surface of the material top view (right) [7]

## 3. Pore network configuration and resulting heat transfer coefficient

As shown on the left hand-side of Figure 1, the pore network is made of an assembly of elemental structures with elemental pore networks assembled upside down. The inlet pores are at the bottom of the structures. Depending on the number of inlets the designed configuration can exhibit one or two pairing levels. Figure 2 depicts the case of dendritic structures with two pores connected to one.

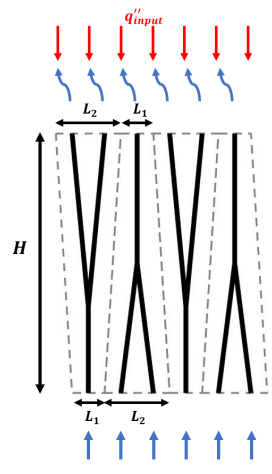


Fig. 2: Example of an assembly of porous structure when N=2 [7].

We investigated various geometrical options in terms of number of inlets and connection level. Results indicate that there are different options to reach identical values of the heat transfer coefficient when the porosity is fixed. For example, the elemental network could be made of two inlets and a large outlet radius, or it could have four inlets and a smaller outer radius. Table 1 shows the results obtained when the outlet pore radius is 0.3 mm with an input heat flux at the top of the pore material  $q''_{input} = 10 \text{ kW/m}^2$ . When there are two inlet pores, the tree-shaped pore network is made of one pairing level, while when the number of inlets is four, the network has two pairing levels. In each case, the numerical procedure allows to determine the radius ratio of the pore channels, their length ratio and angle of bifurcation for minimum friction losses and sufficient capillary force all along the network. Interestingly, for the same porosity, and same outlet pore radius, a

configuration with four inlet channels results in less mass flow rate flowing through the network and evaporating at the top surface of the material. Nevertheless, a higher heat transfer coefficient is obtained to satisfy the energy balance.

Table 1: Results obtained when the elemental system has a fixed porosity and N = 2 or 4 pore inlets.

N, number of inlets	2	4
Heat transfer coefficient, kW/m <sup>2</sup> K	0.72	1.42
Porosity, %	6.32	7.86
$\dot{m}_{total} \times 10^{-8}$ , kg/s	1.38	0.69

#### 4. Conclusion

The objective of the study was to investigate the relationship between the pore network that pulls a heat transfer fluid up by capillary suction to the top of the material where it evaporates, and the obtained heat transfer coefficient. The fundamental approach developed in this work allows to show that for a given porosity it is possible to design the pore network in pore size and connectivity for a targeted heat transfer coefficient. The pore network changes in size in a hierarchical way, leading to a gradient of porosity. The network is made of dendritic elements which geometrical features are deterministic, opening the way to a controlled design of pore networks for controlled heat exchanges by evaporation in the cooling of electronics.

## **Acknowledgements**

Xuewei Zhang thanks the Mechanical Engineering Department of Villanova University for funding her Ph.D. studies.

### References

- [1] D.F. Hanks, Z. Lu, J. Sircar, I. Kinefuchi, K.R. Bagnall, T.R. Salamon, D.S. Antao, B. Barabadi and E.N. Wang, "High heat flux evaporation of low surface tension liquids from nanoporous membranes", *ACS Appl Mater Interfaces*, vol. 12, pp. 7232–7238, 2020.
- [2] S. Anand and C.S. Sharma, "Biomimetic Micropillar Wick for Enhanced Thin-Film Evaporation", *Langmuir*, vol. 39, pp. 6855–6864, 2023.
- [3] Y. Kameya, Y. Takahashi and M. Kaviany, "Surface evaporation enhancement using porous metasurfaces: 3-D multiscale, open-system wick evaporators", *Int J Heat Mass Transf.*, vol. 216, 124605, 2023.
- [4] K.S. Remella and F.M. Gerner, "Separated Liquid-Vapor Flow Analysis in a Mini-Channel with Mesh Walls in the Closed-Loop Two-Phase Wicked Thermosyphon (CLTPWT)", *Energies*, vol. 16, 2023.
- [5] G. Ahmadi, A. Jahangiri and M. Ameri, "The effects of transferred heat and wall material on thermal behaviour of a nano-grooved micro-heat pipe, molecular dynamics simulation", *Eng Anal Bound Elem*, vol. 160, pp. 1–13, 2024.
- [6] P.P. Chakraborty and M.M. Derby, "Analysis of Drying Front Propagation and Coupled Heat and Mass Transfer During Evaporation From Additively Manufactured Porous Structures Under a Solar Flux", *ASME Journal of Heat and Mass Transfer*, vol. 146, pp. 1–13, 2024.
- [7] X. Zhang and S. Lorente, Hierarchical capillary network with graded porosity for evaporative cooling, *Int. Com. Heat and Mass Transfer*, vol. 157, 107757, 2024.